12

Fault Diagnostic of Rotating Machines Based on Artificial Intelligence: Case Studies of the Centrais Elétricas do Norte do Brazil S/A – Eletrobras-Eletronorte

Marcelo Nascimento Moutinho
Centrais Elétricas do Norte do Brasil S/A – ELETROBRAS-ELETRONORTE, Brasil

1. Introduction

The efficiency of the maintenance techniques applied in energy generation power plants is improved when expert diagnosis systems are used to analysis information provided by the continuous monitoring systems used in these installations. There are a large number of equipments available in the power plants of the Centrais Elétricas do Norte do Brazil S/A - ELETROBRAS-ELETRONORTE (known as ELETRONORTE). These equipments operate continuously because are indispensable for the correct functioning of the generation and transmission systems of the company. Anomalies in the operation of these devices can be detected with the use of intelligent diagnosis tools which analysis the information of the continuous monitoring systems and, based in a set of qualitative rules, indicate the best procedures to avoid the fail of the equipments.

The best maintenance strategy used in each equipment operated by ELETRONORTE should consider factors as: equipments importance for the production process, acquisition cost and failure rate. To accomplish this task, one of the three maintenance techniques more used nowadays is chosen: corrective, preventive or predictive [1]. In the predictive maintenance, an operational report of the equipment's condition is emitted using the information collected by the continuous monitoring system. The formulation of such report is a task divided in the following stages: 1) Anomaly identification that can be occurring in the equipment; 2) Detection of the anomalous component; 3) Evaluation of the severity of the fault; and 4) Estimation of the remaining life time of the equipment. The predictive maintenance policies is an efficient practice to identify problems in hydrogenerators that will increase reliability, decrease maintenance costs, limit service failures and increase the life of the machines.

There is a vast literature on techniques for detection and identification of faults known to the FDI (Fault Detection and Isolation). A possible classification of these techniques that consider the aspects related to the type of information available about the process analysis defines three categories: methods based on quantitative models, methods based on qualitative models or semi-qualitative, and methods based on historical data [2]. The first two categories are commonly named Model Based Fault Detection and Isolation (MBFDI) [3].

A MBFDI algorithm consists of two components: the residues generator and the process of decision making: the residues generator compares the current values of inputs, outputs or states of the process with the estimated model that describes the normal behavior; the process decision is the logic that converts the residue signal (quantitative knowledge) on a qualitative information (normal operating condition or abnormal). The bases of MBFDI algorithms are described in [3], [4] and [5]. The main difficulty in implementing a MBFDI algorithm lies in the fact that the fidelity of the model affects the sensitivity of the fault detection mechanism and the diagnosis precision. Many real systems are not susceptible to conventional modeling techniques due to: the lack of precise knowledge about the system, the strongly nonlinear behavior, the high degree of uncertainty, or the time-varying characteristics.

Recently, well successfully applications of predictive techniques have been reported. In [6 to 9] are presented intelligent systems for predictive maintenance addressed to the diagnosis in real-time of industrial processes. In [10] a fault detection and isolation scheme of sensor and actuator is presented. The project considers multivariate dynamic systems with uncertainties in the mathematical model of the process. Detailed studies on the robustness of anomalous systems of identification in presence of modeling errors is also reported in the survival paper [2].

Nowadays, the expert diagnosis technologies available in the market are in maturation process. The tools commercially available have restrictions in the information exchange with the company's legacy systems. The users normally can't change the software structure and don't know the conceptual data base model. Due to these limitations, the company who uses this kind of paradigm is in a difficult situation when software modifications, not considered in the initial project, are necessary to adjust it to a specific application.

In this chapter is described the procedures for designing and test MBFDI system. Two types of models will be used: autoregressive models and fuzzy models. The proposed system is evaluated experimentally using real monitoring data from a synchronous compensator and a synchronous generator. The synchronous compensator analyzed is in operation at Vila do Conde substation, located at Pará state, Brazil. The synchronous generator studied is in operation at Tucuruí Hydroelectric, located at Pará state too. Both equipments are operated by ELETRONORTE.

2. Fuzzy system and regression models for use in diagnosis systems

To design the fault detection system proposed in this work mathematical models are used to describe the relationships between the variables monitored in the equipment analyzed. Two types of models will be used: autoregressive models and fuzzy models. The purpose of this section is describe the two structures used.

2.1 System identification with regression models

The following structure, known in literature as Autoregressive model with exogenous inputs (ARX), will be used [14]:

$$\begin{aligned} &y(t) + a_1 y(k-1) + \ldots + a_{n_a} y(k-n_a) = \\ &b_0 u(k-d) + b_1 u(k-1-d) + \ldots + b_{n_b} u(k-d-n_b) \end{aligned} \tag{1}$$

where $y(k)$ and $u(k)$ are, respectively, the values of the output and input signals at the discrete time k, an integer multiple of the sampling interval T_s, n_a and n_b are the number of regressors is the output and input signals, respectively, and $d \geq 1$ is the output transport system delay as an integer multiple of the sampling interval. Using the discrete delay operator, (q^{-1})[1] , the following polynomial representation of Eq. (1) can be obtained:

$$A(q^{-1})y(t) = q^{-d}B(q^{-1})u(t) \tag{2}$$

where $A(q^{-1})$ and $B(q^{-1})$ are as follow:

$$A(q^{-1}) = 1 + a_1 q^{-1} + a_2 q^{-2} + ... + a_{n_a} q^{-n_a} \tag{3}$$

$$B(q^{-1}) = b_0 + b_1 q^{-1} + b_2 q^{-2} + ... + b_{n_b} q^{-n_b} \tag{4}$$

It is interesting to add stochastic characteristics in the model representing as realistically as possible the nature of the process. This can be done considering that the output signal is affected by uncorrelated noise. Thus, the following representation can be obtained:

$$y(k) = \phi^T(k)\theta(k) + e(k) \tag{5}$$

where $e(k)$ is a Gaussian white noise; $\phi(k)$ is the vector of regressors and $\theta(k)$ is the vector of model parameters. The vectors $\phi(k)$ and $\theta(k)$ are represented as follows:

$$\phi(k) = \left[-y(k-1) \ ...- y(k-n_a) \ u(k-d) \ ... \ u(t-d-n_b) \ \right]^T \tag{6}$$

$$\theta(t) = \left[a_1 \ a_2 ... \ a_{n_a} \ b_0 \ b_1 ... \ b_{n_b} \right]^T \tag{7}$$

The non-recursive least squares method [14] will be used in order to estimate the vector $\hat{\theta}(k)$, which represents approximately the parameter vector $\theta(k)$ of Eq. (5). The objective of the method is to minimize the sum of the squares of the prediction error between the estimated model output and the real output of the plant. Substituting in equation (5) k = 1,2, .., N, we obtain, in matrix notation:

$$\mathbf{y} = \begin{bmatrix} y(1) \\ y(2) \\ \vdots \\ y(N) \end{bmatrix}, \mathbf{\Phi} = \begin{bmatrix} \phi(1)^T \\ \phi(2)^T \\ \vdots \\ \phi(N)^T \end{bmatrix}, \varepsilon = \begin{bmatrix} \xi(1) \\ \xi(2) \\ \vdots \\ \xi(N) \end{bmatrix} \tag{8}$$

$$\mathbf{y} = \mathbf{\Phi}\hat{\theta} + \boldsymbol{\varepsilon} \tag{9}$$

where. $\xi(k) = y(k) - \phi^T(k)\hat{\theta}$. The following quadratic performance index must be minimized:

[1] Represented as follows $q^{-1}y(k) = y(k-1)$

$$J(\hat{\theta}) = \frac{1}{2}\sum_{k=1}^{N} \xi(t)^2 \tag{10}$$

The value of $\hat{\theta}$ that minimizes the Eq. (10) is [15]:

$$\theta_{MQ} = (\mathbf{\Phi}^T\mathbf{\Phi})^{-1}\mathbf{\Phi}^T\mathbf{y} \tag{11}$$

2.2 Identification of predictive models based on fuzzy logic

In this subsection the structure of the fuzzy model used in this work will be described. The following discrete nonlinear system representation is used:

$$y(k) = f\left[\Psi(k-1)\right] \tag{12}$$

where f(.) is a nonlinear function of the *Information Vector* Ψ, defined as:

$$\Psi(k-1) = \left[y(k-1)\cdots y(k-n_a)\ldots u(k-d)\ldots u(k-d-n_b)\right]^T \tag{13}$$

where: n_a and n_b represent the number of regressors of discrete output signals, $y(k)$ and input $u(k)$, respectively, d is the output transport delay as an integer multiple of the sampling interval T_s; e(k) is a random signal that supposedly corrupts the signals of the model is designed in a stochastic environment. This model is known as Non-linear Auto-regressive with exogenous inputs (NARX).

We consider the existence of a measurable set of variables that characterize the operating conditions of the system (12) at every moment. Using these variables, you can define a set of rules that describe, approximately, the behavior of the function $y(k)$:

$$\mathrm{R}^{(l)}\text{: } \mathbf{IF} < V_1 \text{ is } V_{1,i}^l > \mathbf{AND} < V_2 \text{ is } V_{2,j}^l > \mathbf{AND} \ldots \mathbf{AND} < V_k \text{ is } V_{k,p}^l > \mathbf{THEN}\ y_l(k) = f_l(k) \tag{14}$$

where: l=1,2, ..., M; i = 1,2, ..., n_1; j = 1,2, ..., n_2; and p = 1,2,..., n_k. The terms, V_1, V_2, ..., V_k are fuzzy linguistic variables that are part of the vector Ψ and were chosen to describe the system (12). The domain of these variables is uniformly partitioned into n_i = n_1, n_2, ..., n_k fuzzy sets (for example, the partitions of V_i are: $V_{i,1}$, $V_{i,2}$, ..., $V_{i,ni}$. In this work the function f_l(.) is represented by the following linear combination:

$$f_l(k) = c_l^0 + c_l^1 V_1 + c_l^2 V_2 + \cdots + c_l^k V_k \tag{15}$$

onde c_l^i i=1,2,...,k are coefficients to be estimated.

At a given instant of discrete time k each linguistic variable, V_i, will have a membership value $\mu_{V_{i,j}}[V_i\ (t)]$ associated with the fuzzy set j (j = 1,2, ..., n_i). For mathematical simplicity, the membership functions used to represent these sets are triangular and trapezoidal, with the trapezoidal used only in two extreme sets, as shown in Figure 2. It is easy to see that, for each fuzzy variable, at most two and at least one fuzzy set has a membership value different from zero and the sum of these values always is equal one.

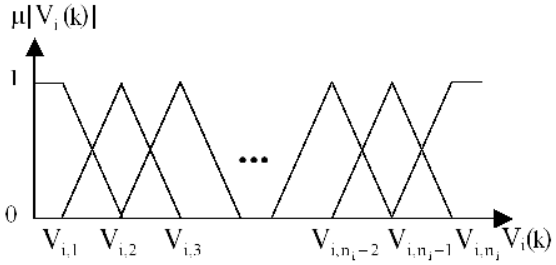

Fig. 2. Membership functions of the n_i fuzzy sets associated with the Linguistic variable $V_i(k)$.

The set of M rules defined by (14) describe a fuzzy system of Sugeno [16], a mathematical tool that can represent globally and approximately the system described in Eq (12). It is a universal nonlinear approximator, a mathematical function that represents with an arbitrary degree of precision, dynamic systems governed by nonlinear relationships.

According to the theory of fuzzy systems [16], the output signal $\hat{y}(k)$ of the fuzzy system defined by the set of rules (14) is obtained by weighted average of the individual outputs of each of the M rules:

$$\hat{y}(k) = \frac{\sum_{l=1}^{M} \omega_l y_l(k)}{\sum_{l=1}^{M} \omega_l} \tag{16}$$

The weights, ω_l, are called Functions Validation. They are calculated in terms of the vector Ψ as follows:

$$\omega_l = \mu_{V_{1,i}^l}(V_1(t)) \times \mu_{V_{2,j}^l}(V_2(t)) \times \cdots \times \mu_{V_{k,p}^l}(V_k(t)) \tag{17}$$

According to Eq.(16), the value of the signal output of the model is a function of the ω_l weights and functions $f_l(.)$. Therefore, for a given set of values of signal $y(k)$ can be found an optimal setting of the parameters of fuzzy membership functions defined on each input and the parameters of the functions $f_l(.)$ that minimizes the difference $y(k) - \hat{y}(k)$ for the entire set. The details of the procedure for identification of these parameters will be the subject matter of section IV which will be described a procedure for identifying models based on real data from a continuous monitoring system described in the next section.

2.3 Prediction techniques based on Adaptive-Network-based Fuzzy Inference Systems (ANFIS)

2.3.1 Synchronous compensator monitoring system – VIBROCOMP

This monitoring system was designed as predictive maintenance tool for Synchronous Compensators (SC). These equipments are large rotary machines of 150 MVAr where the constant evaluation of its physical parameters is critical. In the State of Pará, Eletronorte operates three SC that are part of its transmission system: two are installed in Vila do Conde substation, located in Para State, and one is installed in the Marabá substation. These three

equipments are monitored by VibroComp. Figure 3 shows a photograph of CPAV-01, one of SC monitored in the substation of Vila do Conde. This equipment, a member of the National Interconnected System (SIN), is used for voltage regulation. The main features of CPAV-01 are presented in Table 1.

Fig. 3. Synchronous Compensator 01 of the substation Vila do Conde.

Characteristics	Value
Power	150 MVAR
Speed	900 RPM
Voltage	13.8 KV
Current	6.275 A
Frequency	60Hz

Table 1. Nominal Characteristics of CPAV-01.

The VibroComp system consists of the following parts:

1. *Hardware:*
   - Sources, sensors, transmitters and signal conditioners;
   - Aquisition Computers, Database Computers, data acquisition cards, serial cards, cables, etc..;
2. *Software:*
   - Data Acquisition Module;
   - Database Module;
   - Expert Diagnosis System;
   - Client Module

The signal conditioning hardware and monitoring software were developed at the Centro de Tecnologia da ELETRONORTE, known as the Laboratório Central (LACEN). Further details on the development of VibroComp can be obtained in [17].

To evaluate the operational condition of a SC, mechanical, electrical and thermal properties are monitored. Table 2 shows some of the signs monitored by VibroComp that are used in this work.

Tag	Description	Unit	Type
M_{lah}	Vibr. Bearing Ring - Horizontal	µm	Vibration
M_{laa}	Vibr. Bearing Ring - Axial	µm	Vibration
M_{lav}	Vibr. Bearing Ring - Vertical	µm	Vibration
M_{lbh}	Vibr. Pump Bearing - Horizontal	µm	Vibration
M_{lba}	Vibr. Pump Bearing - Axial	µm	Vibration
M_{lbv}	Vibr. Pump Bearing - Vertical.	µm	Vibration
L_{dh1}	Vibr. Left - Horizontal 1	µm	Vibration
L_{eh2}	Vibr. Left - Horizontal 2	µm	Vibration
P_{h2}	Pressure of Cooling Hydrogen	bar	Pressure
R_{ot}	Compensator Speed	RPM	Speed
P	Active Power	MW	Power
Q	Reactive Power	MVAR	Power
T_{bea87}	Temp. stator bars - slot 87	Cº	Temperature
T_{bea96}	Temp. stator bars - slot 96	Cº	Temperature
T_{bea105}	Temp. stator bars - slot 105	Cº	Temperature
T_{aer}	Temp. Cooling Water - Input	Cº	Temperature
T_{hsr}	Temp. Cooling Hydrogen - Output	Cº	Temperature
T_{her}	Temp. Cooling Hydrogen - Input	Cº	Temperature

Table 2. Some signals monitored by VibroComp.

The Data Acquisition Module is a client/server application that uses the TCP/IP protocol to send information to the Client Module and Database Module. The Client Module was developed in order to be the interface between the user and the Acquisition and Database modules. The client can get the waveforms of the measured signals from the acquisition module and also make the trend analysis and event analysis. The Expert Diagnosis System is used to analyze the information stored in the Database Module. The application runs on the client module and provides to the analyst the possibility of each fails of the equipment. To do this is used a Fuzzy Inference Engine. In Figures 4 and 5 some of the interfaces of VibroComp are presented.

In the next section will present the procedure for the identification of predictive models used in this work. The modeling techniques presented in section II will be used.

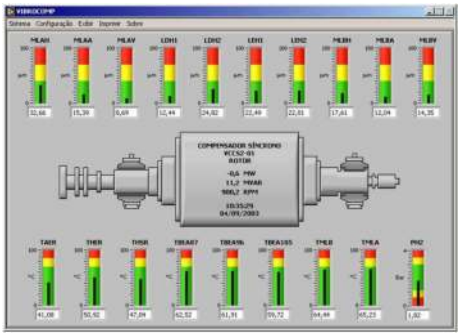

Fig. 4. Main Interface of Client Module of VibroComp

Fig. 5. Interface of the Expert Diagnosis System of VibroComp

3. Case studies 1: System modeling of a synchronous compensator

3.1 Synchronous compensator predictive models

In this section we present a case study where we identified the parameters of mathematical models that describe, approximately, the behavior of a SC operating in a normal condition.

The equipment CPAV-01, located in the Vila do Conde substation was examined. The models proposed in this work were estimated and validated with real data from the VibroComp monitoring system. The analyzed period was 03/01/2008 to 25/03/2008. The SC was under normal conditions without showing any anomaly.

The identification of mathematical models to describe the behavior of CPAV-01 in this period is a practical procedure that can be divided into the following steps:

1. Statistic analysis of the monitored signals to identify dynamic relationships;
2. Choose the structure of the models;
3. Models Estimation and validation;

The objective of the first step is to identify the correlations that exist in the monitored signals. In this work two mathematical functions are used: Autocorrelation Function (ACF) and Cross-Correlation Function (CCF):

The ACF was used to identify correlations in time of a discrete signal $y(k)$. The formulation used is as follows:

$$r_\tau = \frac{\sum_{k=\tau+1}^{N}[y(k)-\bar{y}][y(k-\tau)-\bar{y}]}{\sum_{k=1}^{N}[y(k)-\bar{y}]^2} \tag{18}$$

where: $\bar{y}$ is the average value of the signal $y(k)$ and k is the discrete time, an integer multiple of the sampling interval, T_s.

The ACF analysis revealed that some of the monitored signals ($P(k)$ and $R_{ot}(k)$) behaves approximately like random and uncorrelated white noise. Other signs ($T_{aer}(k)$, $P_{h2}(k)$, $M_{lah}(k)$, $P(k)$, $T_{bea87}(k)$ and $L_{dh1}(k)$) are auto-correlated and can be characterized by models with Auto-

regressive Moving Average (ARMA) [18]. The profile of the ACF shows signs of a fixed pattern for the first time delays followed by a pattern composed of combinations of exponential and damped sinusoidal functions. In Figure 6, for example, is shown the profile of the auto-correlation signal $T_{bea87}(k)$.

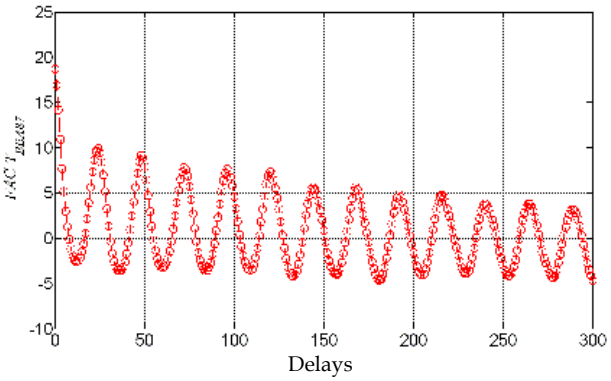

Fig. 6. Profile Auto-correlation function of the signal $T_{bea87}(k)$.

The CCF is used to assess correlations between two discrete signals $u(k)$ and $y(k)$. The following formulation was used:

$$r_{yu} = \frac{\sum_{k=\tau+1}^{N}[y(k)-\bar{y}][u(k-\tau)-\bar{u}]}{\sum_{k=1}^{N}[y(t)-\bar{y}]^2} \tag{19}$$

where $\bar{u}$ is the average value of the signal u(k).

In the Figure 7 is presented the profile of the CCF between the signal $T_{aer}(k)$ and the signal $T_{bea87}(k)$. The analysis of the CCF of the $T_{aer}(k)$ indicates that this signal is more correlated to the signs $T_{bea87}(k)$, $P_{h2}(k)$ and $Q(k)$.

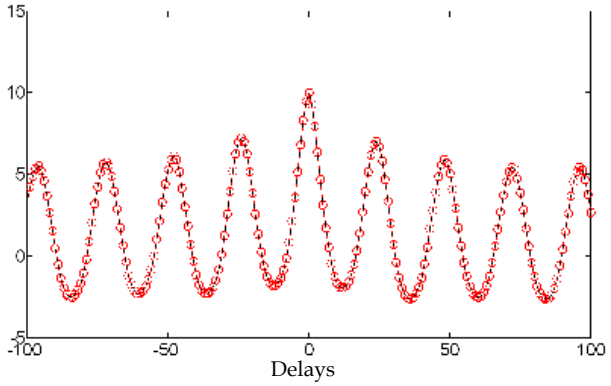

Fig. 7. Profile of the cross-correlation function between the signal $T_{aer}(k)$ and the signal $T_{bea87}(k)$.

A similar analysis realized for the signal $T_{aer}(k)$ was performed for all other signs in Table 2. The final result of the statistic analysis is presented in Table 3. The interpretation of this table is as follows: the signals in the left column are related to the central column signals at delays intervals specified in the right column. For example, the signal $T_{aer}(k)$, is self-correlated and is also related with the signs $T_{bea87}(k)$, $T_{bea87}(k\text{-}1)$, $P_{h2}(k\text{-}1)$, $P_{h2}(k\text{-}2)$, $P_{h2}(k\text{-}3)$ and so on. The order of presentation of the signs in the center column is proportional to the intensity of the relationship with the signals in the left column.

Tag	Correlations	Delays
L_{dh1}	M_{lah}, T_{bea87} e L_{eh2}	[1 7], [1 7] e [1 7]
P_{h2}	Q, T_{bea87} e T_{aer}	[1 3], [1 3] e [1 3]
Q	P_{h2}, T_{bea87} e T_{hsr}	[1 3], [1 2] e [1 3]
T_{bea87}	T_{bea105}, Q, e T_{her}	[1 2], [1 2] e [1 2]
T_{aer}	T_{aer}, T_{bea87}, P_{h2}, Q	[1 4], [0 2], [0 2] e [0 2]

Table 3. Correlations of Signals Monitored by VibroComp.

The choice of the model structure, the goal of the second step of the identification procedure was based on information in Table 3. The statistical characteristics of the signals indicate that Auto-regressive Moving Average with Exogenous Input (ARMAX) models are good alternatives to explain the dynamic relationships of the monitored signals. However, it is suspected that there are nonlinear relationships between the monitored signals. These relationships are better described by a universal nonlinear approximate operator. For comparison purposes in this paper will be use three types of mathematical models: Single-input single-output (SISO) ARMAX, multi-inpult single-output (MISO) ARX and a MISO Sugeno fuzzy system. For exemplification purposes, details of the procedure for identification of the $T_{aer}(k)$ model will be presented. The other signs presented in Table 3. can be estimated by a similar procedure.

The first model analyzed for the sign $T_{aer}(k)$ is the SISO ARMAX with the following structure:

$$T_{aer}(k)=\sum_{i=1}^{4} a_i T_{aer}(k-i)+\sum_{i=0}^{1} b_i T_{bea87}(k-i)+\varepsilon(k)+c_1\varepsilon(k-1) \tag{20}$$

where ε is an uncorrelated noise that supposedly corrupts the data, since the model is designed in a stochastic environment. For the sake of structural simplicity, only the signal $T_{bea87}(k)$ was chosen as the input for this model. As shown in Table 3, this signal has higher values for the CCF with the $T_{aer}(k)$. Under an intuitive point of view, it is coherent to suppose that the temperature of cooling water is dependent on the temperature values of the stator bars of SC.

A second more complex MISO ARX model was proposed to explain the behavior of the signal $T_{aer}(k)$. In this case, the other relationships identified in Table 3 were used. The following structure was chosen:

$$
\begin{aligned}
A(q^{-1})y(k) &= B(q^{-1})U(k) + \varepsilon(k) \\
y(k) &= T_{aer}(k) \\
U(k) &= \left[\, P_{h2}(k)\ T_{bea87}(k)\ Q(k) \right]^T \\
A(q^{-1}) &= 1 + a_1 q^{-1} + a_2 q^{-2} + a_3 q^{-3} + a_4 q^{-4} \\
B(q^{-1}) &= \left[B_0(q^{-1}) + B_1(q^{-1}) + B_2(q^{-1}) \right] \\
B_0(q^{-1}) &= b_{00} + b_{01} q^{-1} + b_{02} q^{-2} \\
B_1(q^{-1}) &= b_{10} + b_{11} q^{-1} + b_{12} q^{-2} \\
B_2(q^{-1}) &= b_{20} + b_{21} q^{-1} + b_{22} q^{-2}
\end{aligned}
\tag{21}
$$

The third model proposed model uses a fuzzy inference system to represent the signal $T_{aer}(k)$. Table 4 presents details of the two topologies used. All models are Sugeno fuzzy systems with weighted average defuzzifier and number of outputs equal to the number of rules.

Inputs	Sets	Function	Parameters
Fuzzy Model Topology 1: MFT1			
T_{aer}, T_{bea87}	2-3	*Bell*	50 ou 135
Fuzzy Model Topology 2: MFT2			
T_{aer}, T_{bea87}, P_{h2}	2-3	*Gaussiana*	44 ou 96
Fuzzy Model Topology 3: MFT3			
T_{aer}, T_{bea87}	2	*Gaussian*	212

Table 4. Structure of Fuzzy Models for Signal $T_{aer}(k)$

The nomenclature used to identify the models is as follows: *MFT1* represents the Fuzzy Model Topology 1. The interpretation of other fields in the Table 4 is as follows: in each model are specified the inputs, the number of sets on each input and the type of membership function. The model *MFT1*, for example, uses two inputs with two or three Bell fuzzy sets in each input. The number of parameters in the model is 50 or 135, depending on the chosen combination. The Bell and Gaussian function used are as follows.

$$
f_{Bell}(x,a,b,c) = \frac{1}{1 + \left| \frac{x-c}{a} \right|^{2b}} \tag{22}
$$

$$
f_{Gauss}(x,\sigma,c) = e^{\left(\frac{-x+c}{\sqrt{2}\sigma} \right)^2} \tag{23}
$$

The parameter estimation was performed in the MATLAB environment. To estimate the models of the linear equations (20) and (21) we used the System Identification Toolbox [19]. The estimation method used was the non-recursive least squares. The mass of data was divided into two parts: the first was used for the estimation of the model and the second part was used for validation. Figure 8 shows the time domain validation of the model of

Equation (20). The sampling interval used in the model is T_s = 1 hour. The model can explain the dynamics of the signal in most of the time interval analyzed. The identified parameters are presented in the Table 5.

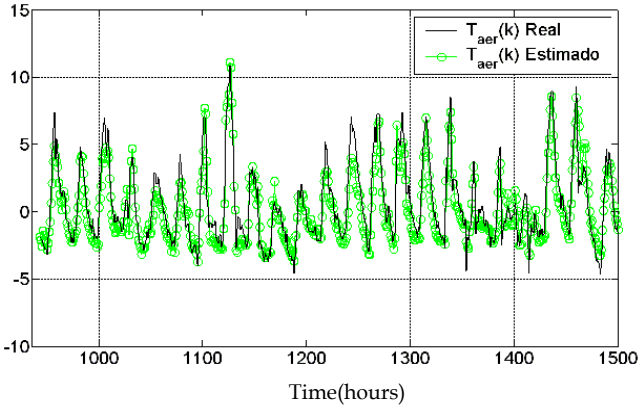

Fig. 8. Comparison between the output signal of the SISO Model and the real signal $T_{aer}(k)$.

Parameters	Values	Parameters	Values
a_1	-1.054051	b_0	0.624452
a_2	0.130458	b_1	-0.531587
a_3	0.036976	c_1	-0.296779
a_4	0.016368	-	-

Table 5. Coefficients of the Linear SISO Model for Signal $T_{aer}(k)$.

Figure 9 shows the time domain validation of the MISO model of equation (21). Table 5 shows the values of the estimated coefficients.

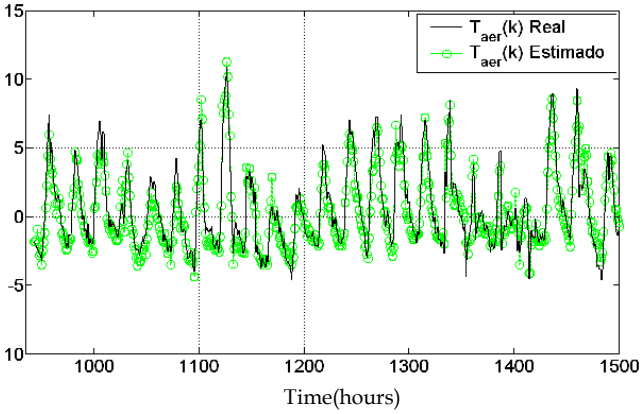

Fig. 9. Comparison between the output signal of the MISO Model and the real signal $T_{aer}(k)$.

Fuzzy models presented in Table 6 were estimated with the algorithm ANFIS (Adaptive-Network-based Fuzzy Inference System) proposed by Jyh-Shing [20] and available on Fuzzy Systems Toolbox of MATLAB, MathWorks (2002). ANFIS is an algorithm for parameter adjustment of Sugeno fuzzy systems based on training data. In Figure 10 presents the results of the comparison between the output of the model *MFT2* and the real signal $T_{aer}(k)$.

Parameters	Values	Parameters	Values
a_1	-0.546560	b_{10}	0.624452
a_2	-0.194398	b_{11}	-0.531587
a_3	-0.031782	b_{12}	-0.296779
a_4	0.035349	b_{20}	-0.024828
b_{00}	0.829278	b_{21}	0.002835
b_{01}	-0.450037	b_{22}	0.013416
b_{02}	-0.145693	-	-

Table 6. Coefficients of the Linear MISO Model for Signal $T_{aer}(k)$.

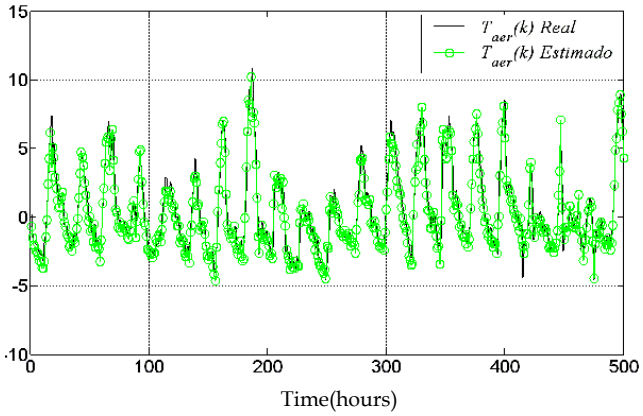

Fig. 10. Comparison between the output signal of the *MFT2* model and the real signal $T_{aer}(k)$.

A similar procedure to that described for the signal $T_{aer}(k)$ was performed for all other signals in Table 3. Annex A shows the identified models. The set of models obtained represents the normal behavior of CPAV-01. Comparing the behavior estimated by the standard model with the actual behavior of the equipment is possible to identify the occurrence of malfunctions. The performance of predictive models of the signal $T_{aer}(k)$ will be presented in the next section.

3.2 Performance evaluation of predictive models

In this section we present the results of performance evaluation of predictive models estimated in Section IV-A. The criteria used are as follows:

- Structural Complexity (SCO);
- Computational Effort for Estimation (CEE);
- Mean Square Error (EMQ);

The Structural Complexity (SCO) can be evaluated by the total number of adjustable parameters. For the fuzzy models the number of rules and membership sets are also considered.

The Computational Effort for Estimation (CEE) can be measured by the number of training epochs until a good model is estimated. In this work the efficiency of the estimation method is not considered. Therefore, a simplifying assumption will be used to assume that the cost estimation is associated only to the number of training epochs until a certain level of accuracy of the model is achieved.

The quality of a model depends on the value of the Mean Square Error Training (EMQ_T) and the Mean Squared Validation (EMQ_V). In this work the following index will be used:

$$EMQ_x = \frac{1}{N}\sum_{k=0}^{N}\left[\hat{T}_{aerx}(k) - T_{aerx}(k)\right]^2 \tag{24}$$

where $\hat{T}_{aerx}(k)$ is the signal is estimated; $T_{aerx}(k)$ is the real measured signal, and $x \in [T\ V]$ indicates the error is calculated with training or validation data.

In the Table 7 are presented the results of the training of the fuzzy models. In some situations the increase in the number of membership functions results in improved performance during the training but decreased performance in the validation. This observation can be proved for the model *MFT1* comparing lines 1 and 2 with lines 3 and 4 and for the model *MFT2* comparing lines 5 and 6 with rows 7 and 8.

The increase in the number of training epochs can also exert a deleterious effect on the EMQ_V. For the model *MFT1*, this effect is observed comparing lines 1 with 2 and 3 with 4. For the model *MFT2* this increase in EMQ_V is observed comparing the line 7 to line 8. The cause of this behavior is to decrease the generalize ability of the model during the training, phenomenon known as overfitting. The best performance in the training was obtained with the model *MFT3* on line 10 and the best performance in the validation phase was observed in line 6 with the model *MFT2*.

Comparing the model MFT3 with the models MFT1 and MFT2 it's observed that increasing the number of inputs improves performance in training data. However, this relationship was not observed when the validation data are analyzed.

The comparison between the models of Equations (20) and (21) shows that the MISO is beter. In this case the increase in the SCO resulted in better performance.

In all simulations the performance of the Fuzzy model was superior to linear models in the training data. However, when the validation data are considered this relationship is not always true. An example is the comparison between lines 12 and 4 where we observe an increase in the SCO and a degradation of performance in the validation data.

ID	Training	EMQ_T	EMQ_V
MFT1			
2 sets, 50 parameters, 8 rules			
1	20	0.7071	1.029
2	150	0.6009	1.231
3 sets, 135 parameters, 27 rules			
3	10	0.4936	3.4069
4	50	0.4762	6.1030
MFT2			
2 sets, 44 parameters, 8 rules			
5	10	0.6597	1.0083
6	250	0.6064	0.9085
3 sets, 96 parameters, 27 regras			
7	10	0.4692	3.8152
8	20	0.4663	4.1179
MFT3			
2 sets, 212 parameters, 32 rules			
9	10	0.3434	4.4351
10	20	0.3405	4.3070
ML1			
0 sets, 7 parameters, 0 rules			
11	1	1.7053	4.4881
ML2			
0 sets, 13 parameters, 0 rules			
12	1	1.2130	3.9079

Table 7. Results of Fuzzy Models Training for the Signal $T_{aer}(k)$.

4. Case studies 2: Development of a Fuzzy expert system for a synchronous compensator

4.1 Project of the fuzzy expert system

This section describes the project of a Fuzzy Expert System used to faults diagnosis of a SC based on a Mandan fuzzy system [16]. The design methodology is formed by the following steps:

1. Selection of input variables - the choice depends on the quantity and quality of information provided by the monitoring system. The cause and effect relationships involved in the operation of the equipment helps in this selection. A detailed study of the correlation between variables can help eliminate redundancy of information simplifying the inference unit;
2. Selection of Output Variables - At this stage the following question must be answered: What are the faults to be detected?
3. Selection of Membership Functions – For each input and output, acceptable and not acceptable levels should be determined. In addition, the number of sets and the overlap must be specified for each variable;

4. Formulation of Rules – Standard fuzzy IF-THEN rules that considers the normality conditions;
5. Selection of Operators – Plausibility and continuity should be used for this selection;
6. Adjust of Rule Base – Simulation using trial and error procedure used to detect inconsistencies in the rule base. Mathematical models of the monitored system also can be used;

In the first stage two approaches have been proposed: the first strategy considers only the global values of the signals monitored by VibroComp as inputs and the second approach uses the spectral information of the vibration signals as inputs. In this paper, only the conventional approach will be used because the data base structure of the Expert System of VibroComp has not using spectrum information. The input signals to be used are: M_{lah}, M_{lav}, M_{laa}, M_{lba}, M_{lbh} and M_{lbv}. A description of these abbreviations can be found in Table 2.

The output variables are the faults to be detected. For each fault the expert maintenance engineers of the company defined default probability values of the fault. Table 8 shows the outputs of the fuzzy expert system and the probabilities values defined.

ID	Fail	Values
F1	Mechanical Unbalance	10%, 20%, 70%, 90%
F2	Faulty bearing	10%, 20%, 70%, 90%
F3	Rubbing Axis	20%, 30%, 50%, 70%
F4	Housing/Support Loose	10%, 20%, 70%, 90%
F5	Oil Whirl	10%, 20%, 70%, 90%
F6	A bent shaft	10%, 30%, 40%, 60%
F7	Misalignment of Bearings	10%, 20%, 30%, 70%

Table 8. Outputs of Synchronous Compensator Fuzzy Expert System

The structure defined in the expert system outputs is so peculiar: for each fault are defined the expected possibilities. The table 8 was determined from the experience of the company's maintenance experts. The validation tests of the fuzzy expert system proposed show that this feature can be better used if each fault is described by a finite number of fuzzy sets equal to the number of possibilities provided by the experts. From a practical point of view, this project choice is based on the following argument: defining a finite number of fault possibilities ensures that the diagnostic system will present expected results.

This project choice, however, does not guarantee the accuracy of the diagnosis. The distribution of fuzzy membership sets in the output variables is a very important aspect of the fuzzy expert system. There are significant inconsistencies between the output values of the fuzzy expert system and the expected values when the membership functions uniformly distributed throughout the universe of discourse of the output variables. So uniformly in the distribution the membership functions, which is a common practice in most applications described in the literature [16], did not show satisfactory results for any kind of defuzzifier used. The solution was to specify non-overlapping fuzzy sets, located in a rather narrow

around the values of precision defined by the expert engineers. Triangular functions with no more than 10% of base showed satisfactory results. Figure 11 is shown an example of distribution of membership functions of the output variable F7. It was observed that this distribution has great influence on the behavior of the diagnostic system.

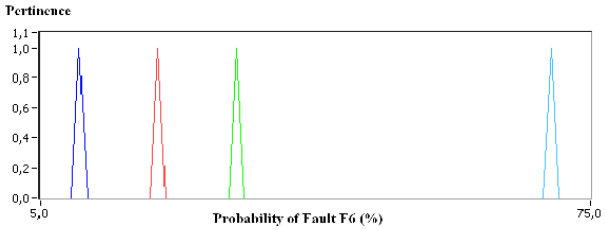

Fig. 11. Membership functions for variable F7, misalignment of bearings.

Fifteen rules were defined by the expert engineers, so that the diagnostic system can detect the faults described in Table 8. These rules use only vibration and temperature variables. Below is one of the specified rules:

Regra 1: IF M_{lah} IS Alarme 1 AND M_{lbh} IS Alarme 1 THEN
F1 IS 70% AND F2 IS 30% AND F3 IS 20% AND F4 IS 10% AND F5 IS 10% AND F6 IS 10% AND F7 IS 20%.

In this and all other rules provided by the experts can be observed another unique feature: the antecedents are short combinations of the monitored signals and the consequents are long combinations of faults. Table 9 shows the characteristics of the membership functions of input variables.

Universe [0 100]	Function	
Fuzzy Sets	Type	Interval
Normal	Trapezoidal	[0 0 30 40]
Alarm - 1	Triangular	[40 45 50]
Alarm - 2	Trapezoidal	[50 60 100 100]

Table 9. Membership Functions of Vibration Inputs: M_{lah}, M_{lav}, M_{laa}, M_{lbh}, M_{lbv} and M_{lba}.

Changes made in the distribution of the membership functions in the output variables and the choice of the precision of the faults resulted in satisfactory performance. In the validation tests were observed differences of performance related to the defuzzifier used. This is a project choice and the most appropriate defuzzifier depends on the application.

The other operators of the inference unit have not great influence on the performance. The Fuzzy Expert System, in its current state of development, allows the use of the following methods: T-Norm, Min operator; Mandani implication and Maximum aggregation method.

4.2 Experimental evaluation of the fuzzy expert system

To evaluate the fault detection methodology proposed in this work will be presented a case study where it was possible to detect an anomalous behavior based on the residual analysis of the reference models of the SC.

In the figure 12 is presented the analyzed event which was monitored by VibroComp on 11/03/2008 11:47:56 AM in CPAV-01 at t = 1560 hours of operation. In this situation was detected a considerable increase in the stator bars temperatures $T_{bea87}(k)$, $T_{bea96}(k)$ and $T_{bea105}(k)$. We also observed an increase in the value of reactive power that reached the value of $Q(k)$ = 148,5 MVAR, close to the nominal limit of apparent power of the equipment (150MVA). In Table 10 are presented the recorded values and the normal limits of each monitored signal. Is note the scope of this work explain the causes of the dynamic behavior observed in CPAV-01 based on laws of physics and mechanical models. To establish clearly these cause and effect relationships, mechanical engineering and dynamic vibration knowhow are required, The author of this article does not have this knowhow. The main objective of this work is not to explain. The intention is to describe the mechanical behavior of the studied system and classify this dynamic in patterns or signatures using mathematical models estimated and validated based on real monitoring data. Using these models a fault detection system is projected based on MBFDI techniques.

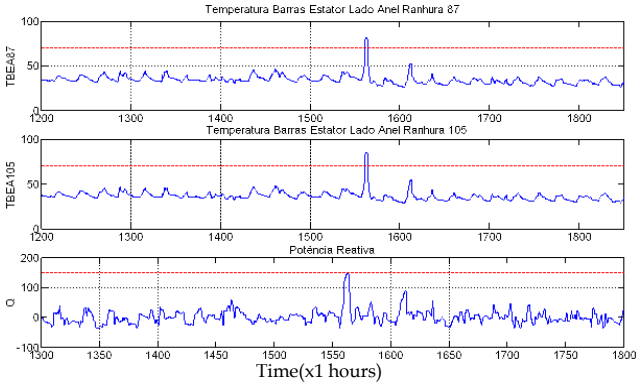

Fig. 12. Experimental evaluation of fuzzy expert system with case study in CPAV-01. Signals monitored during the event and normal limits.

Tag	Value	Limit of Normality
$T_{bea87}(k)$	82ºC	70º C
$T_{bea96}(k)$	82,23ºC	70º C
$T_{bea105}(k)$	82,53ºC	70º C
$Q(k)$	148,5 MVAR	150 MVAR

Table 10. Values monitored by VibroComp during the stator temperature event.

Figures 13 to 15 are presented the results of the analysis of the event using the MBFDI technique presented in this work. *MFT2*, the SISO linear model of Equation (20) and the MIMO linear model of Equation (21) are used as reference models, respectively. In the condition of normality, the residual signal has a mean near zero and a low standard

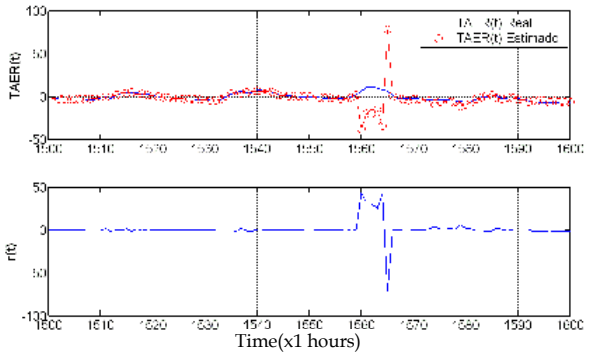

Fig. 13. Increase in the stator bars temperatures - Results of the event analysis using the MBFDI technique with Fuzzy *MFT*2.

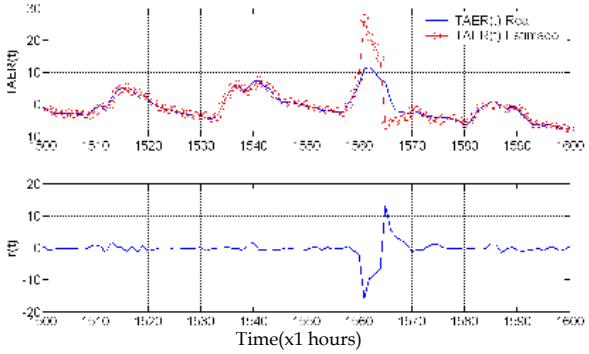

Fig. 14. Increase in the stator bars temperatures - Results of the event analysis using MBFDI technique with the SISO linear model.

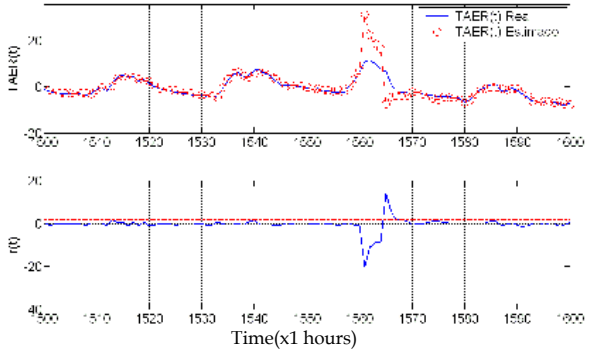

Fig. 15. Increase in the stator bars temperatures - Results of the event analysis using MBFDI with MISO Linear Model.

deviation. At the beginning of the anomalous behavior, the residues signal increases in the three models, which allows a rapid and reliable detection of the failure. In the model the

increase is greater *MFT2* indicating that this model has a higher sensitivity for the detection of such failures. The two linear models have approximately the same level of residue during the event.

One of the rules used for the residues evaluation is shown:

$$\begin{gathered}\text{IF } (|r(k)| > r_{Taer}) \text{ AND } (T_{bea87}(k)_{\,Real} > LT) \\ \text{THEN} \\ \text{FAILURE = Stator Temperature out of Range} \\ r(k) = T_{aer}(k) \text{ Real } - \; T_{aer}(k)_{\,Estimated}\end{gathered} \tag{25}$$

where: $r(k)$ represents the residual of signal $T_{aer}(k)$; r_{Taer} is the maximum allowed residue in the normal condition, and LT represents the thermal limit of the stator winding.

5. Conclusions

In this paper we presented the design and experimental evaluation of a MBFDI system used for SC. The predictive models used in the proposed system were estimated based on real data obtained from the monitoring of the studied equipment during normal conditions. With these models is still possible to detect failures in a fledgling state from the comparison between model output and real signs monitored, as was presented in a case study where it was possible to detect the moment of occurrence of a failure.

6. Appendix A: Structure of the models of the signs *Mlah*, *Ldh1*, *Ph2*, *Q*, *Tbea87*

The structure of the SISO linear model for the signal T_{bea87} is as follows:

$$T_{bea87}(k) = \sum_{i=1}^{4} a_i T_{bea87}(k-i) + \sum_{i=0}^{3} b_i T_{bea105}(k-i) + \varepsilon(k) + c_1 \varepsilon(k-1) \tag{26}$$

In the figure 16 is presented the results of the estimation of the SISO model of Eq. (26).

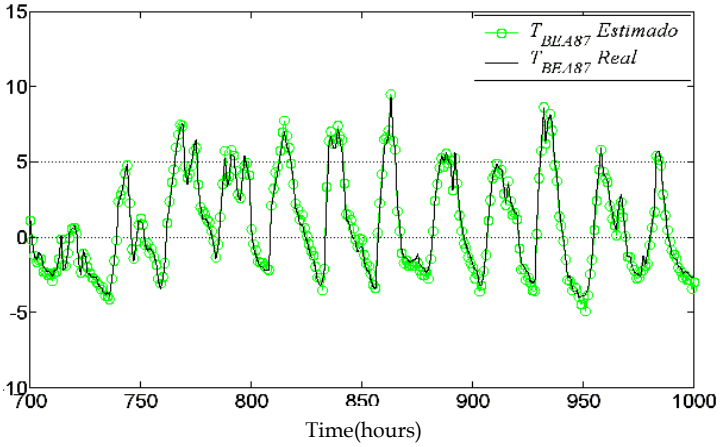

Fig. 16. Comparison between the signal estimated by the linear SISO model and the real signal $T_{bea87}(k)$.

The structure of the MISO linear model for the signal T_{bea87} is as follows:

$$\begin{aligned} A(q^{-1})y(k) &= B(q^{-1})U(k) + \varepsilon(k) \\ y(k) &= T_{bea87}(k) \\ U(k) &= \left[T_{bea105}(k)\ T_{her}(k)\ \ Q(k) \right]^T \\ A(q^{-1}) &= 1 + a_1 q^{-1} + a_2 q^{-2} + a_3 q^{-3} + a_4 q^{-4} \\ B(q^{-1}) &= \left[B_0(q^{-1}) + B_1(q^{-1}) + B_2(q^{-1}) \right] \\ B_0(q^{-1}) &= b_{00} + b_{01} q^{-1} + b_{02} q^{-2} \\ B_1(q^{-1}) &= b_{10} + b_{11} q^{-1} + b_{12} q^{-2} \\ B_2(q^{-1}) &= b_{20} + b_{21} q^{-1} + b_{22} q^{-2} \end{aligned} \tag{27}$$

In the figure 17 is presented the results of the estimation of the MISO model of Eq. (27).

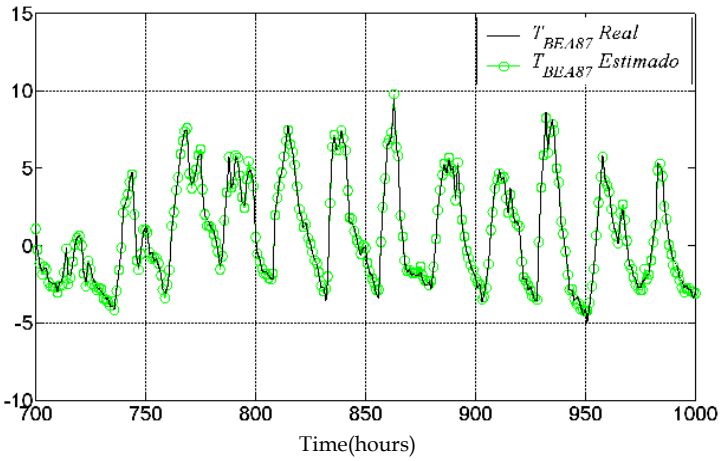

Fig. 17. Comparison between the signal estimated by the linear MISO model and the real signal $T_{bea87}(k)$.

The structure of the SISO linear model for the signal $Q(k)$ is as follows:

$$Q(k) = \sum_{i=1}^{7} a_i Q(k-i) + \sum_{i=0}^{1} b_i T_{bea87}(k-i) + \varepsilon(k) + c_1 \varepsilon(k-1) \tag{28}$$

In the figure 18 is presented the results of the estimation of the SISO model of Eq. (28).

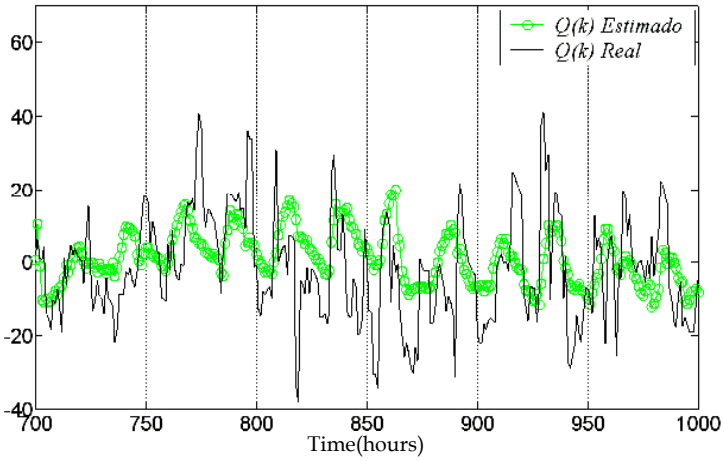

Fig. 18. Comparison between the signal estimated by the linear SISO model and the real signal $Q(k)$.

The structure of the MISO linear model for the signal $Q(k)$ is as follows:

$$
\begin{aligned}
A(q^{-1})y(k) &= B(q^{-1})U(k) + C(q^{-1})\varepsilon(k) \\
y(k) &= Q(k) \\
U(k) &= \left[T_{bea87}(k)\ T_{aer}(k)\ \ T_{hsr}(k) \right]^T \\
A(q^{-1}) &= 1 + a_1 q^{-1} \\
B(q^{-1}) &= \left[B_0(q^{-1}) + B_1(q^{-1}) + B_2(q^{-1}) \right] \\
B_0(q^{-1}) &= b_{00} + b_{01} q^{-1} + b_{02} q^{-2} \\
B_1(q^{-1}) &= b_{10} + b_{11} q^{-1} + b_{12} q^{-2} \\
B_2(q^{-1}) &= b_{20} + b_{21} q^{-1} + b_{22} q^{-2} \\
C(q^{-1}) &= 1 + c_1 q^{-1} + c_2 q^{-2}
\end{aligned}
\tag{29}
$$

In the figure 19 is presented the results of the estimation of the MISO model of Eq. (29).

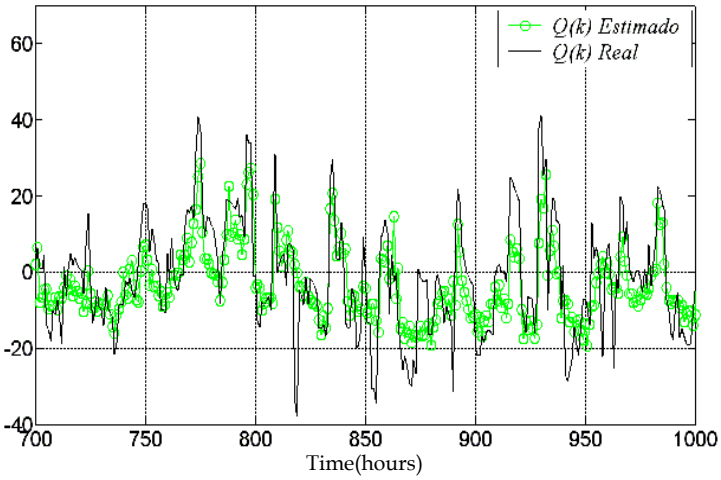

Fig. 19. Comparison between the signal estimated by the linear MISO model and the real signal $Q(k)$.

The structure of the SISO linear model for the signal $P_{h2}(k)$ is as follows:

$$P_{h2}(k)=\sum_{i=1}^{5} a_i P_{h2}(k-i)+\sum_{i=0}^{8} b_i T_{aer}(k-i)+\varepsilon(k)+c_1\varepsilon(k-1) \quad (30)$$

In the figure 20 is presented the results of the estimation of the SISO model of Eq. (30).

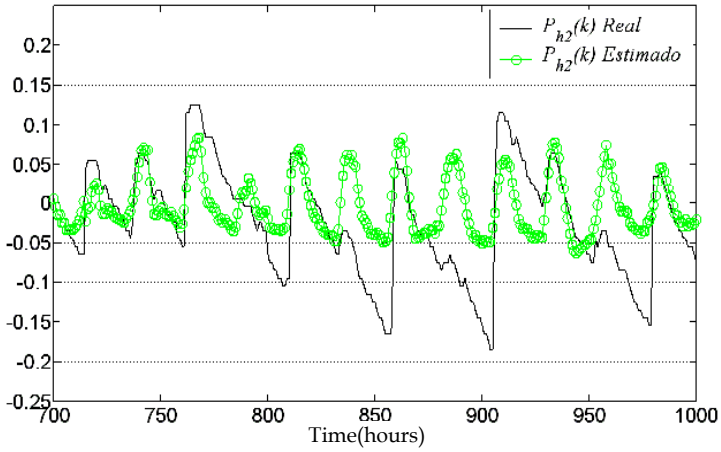

Fig. 20. Comparison between the signal estimated by the linear SISO model and the real signal $P_{h2}(k)$.

The structure of the MISO linear model for the signal $P_{h2}(k)$ is as follows:

$$
\begin{aligned}
A(q^{-1})y(k) &= B(q^{-1})U(k)+\varepsilon(k)\\
y(k) &= P_{h2}(k)\\
U(k) &= \left[\, Q(k)\; T_{bea87}(k)\; T_{aer}(k)\right]^T\\
A(q^{-1}) &= 1+a_1q^{-1}\\
B(q^{-1}) &= \left[\, B_0(q^{-1})+\, B_1(q^{-1})+\, B_2(q^{-1})\right]\\
B_0(q^{-1}) &= b_{00}+b_{01}q^{-1}+b_{02}q^{-2}+b_{03}q^{-3}\\
B_1(q^{-1}) &= b_{10}+b_{11}q^{-1}+b_{12}q^{-2}+b_{13}q^{-3}\\
B_2(q^{-1}) &= b_{20}+b_{21}q^{-1}+b_{22}q^{-2}+b_{23}q^{-3}
\end{aligned}
\tag{31}
$$

In the figure 21 is presented the results of the time comparison of the estimated MISO model of Eq. (31).

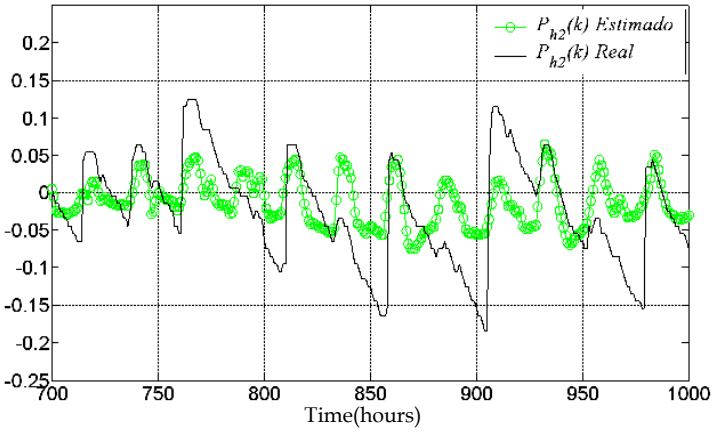

Fig. 21. Comparison between the signal estimated by the linear MISO model and the real signal $P_{h2}(k)$.

The structure of the SISO linear model for the signal $L_{dh1}(k)$ is as follows:

$$
\begin{aligned}
L_{dh1}(k) = &\sum_{i=1}^{2} a_i L_{dh1}(k-i)+\sum_{i=0}^{2} b_i T_{bea87}(k-i)+\\
&+\varepsilon(k)+\sum_{i=1}^{2} c_i \varepsilon(k-1)
\end{aligned}
\tag{32}
$$

The structure of the MISO linear model for the signal $L_{dh1}(k)$ is as follows:

$$
\begin{aligned}
A(q^{-1})y(k) &= B(q^{-1})U(k)+\varepsilon(k)\\
y(k) &= L_{dh1}(k)\\
U(k) &= \left[\ T_{bea87}(k)\ \ M_{lah}(k)\ L_{eh2}(k)\right]^T\\
A(q^{-1}) &= 1+a_1q^{-1}\\
B(q^{-1}) &= \left[\ B_0(q^{-1})+\ B_1(q^{-1})+\ B_2(q^{-1})\right]\\
B_0(q^{-1}) &= \sum_{i=0}^{7} b_{0i}q^{-i}\\
B_1(q^{-1}) &= \sum_{i=0}^{7} b_{1i}q^{-i}\\
B_2(q^{-1}) &= \sum_{i=0}^{7} b_{2i}q^{-i}
\end{aligned}
\tag{33}
$$

In the figures 22 and 23 are presented the results of the time comparison of the estimated SISO and MISO models Eq. (32) and Eq. (33).

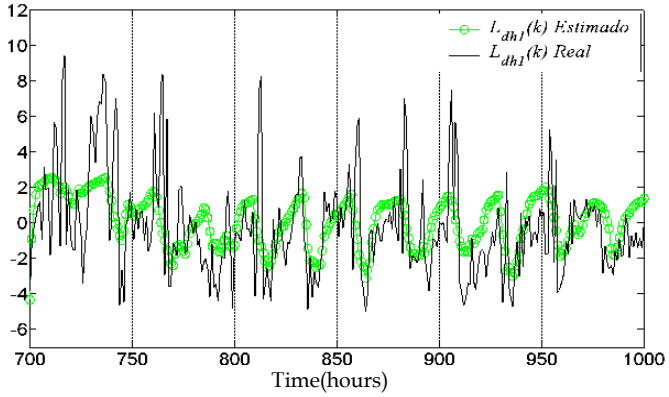

Fig. 22. Comparison between the signal estimated by the linear SISO model and the real signal $L_{dh1}(k)$.

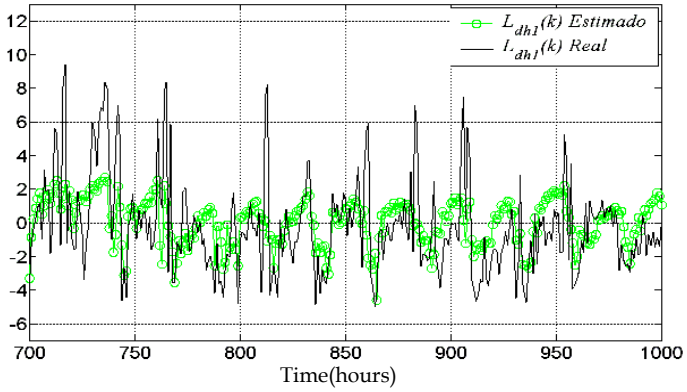

Fig. 23. Comparison between the signal estimated by the linear MISO model and the real signal $L_{dh1}(k)$.

7. References

[1] Nepomuceno, L. X.; *Técnicas de Manutenção Preditiva*; Editora Edgard Blücher Ltda; Volume 2; 1989

[2] Venkat Venkatasubramanian, Raghunathan Rengaswamy, Kewen Yin, Surya N. Kavuri; *A review of process fault detection and diagnosis Part I: Quantitative model-based methods*. Computers and Chemical Engineering, 27, 2003, 293-311.

[3] Patton, R. J., Frank, P. M., and Clark, R. N.; *Fault Diagnosis in Dynamic Systems, Theory and Application*. Control Engineering Series. Prentice Hall, London 1989.

[4] Chen, J. and Patton, R. J. *Robust Model Based Fault Diagnosis for Dynamic Systems*. Kluwer Academic, 1999.

[5] Basseville, M. and Nikiforov, I. V. *Detection of Abrupt Changes: Theory and Application*. Prentice Hall, 1993.

[6] Mari Cruz Garcia, Miguel A. Sanz Bobi and Javier del Pico *SIMAP - Intelligent System for Predictive Maintenance Application to the health condition monitoring of a windturbine gearbox*, Elsevier, Computers in Industry, vol 57, 2006, 552568;

[7] Moutinho, Marcelo N. *Sistema de Análise e Diagnóstico de Equipamentos Elétricos de Potência - SADE*. II Semana Eletronorte do Conhecimento e Inovação (II SECI). 21 a 23 de outubro de 2009, São Luís - MA.

[8] Moutinho, Marcelo N. *Fuzzy Diagnostic Systems of Rotating Machineries, some ELETRONORTE's applications*. The 15th International Conference on Intelligent System Application to Power Systems, Curitiba - Brazil, 2009.

[9] Moutinho, Marcelo N. *Classificação de Padrões Operacionais do Atuador Hidráulico do Distribuidor de um Hidrogerador Utilizando Técnicas de Estimação Paramétrica e Lógica Fuzzy - Resultados Experimentais*. XIX SNPTEE - Seminário Nacional de Produção e Transmissão de Energia Elétrica. Florianópolis, SC. 23 a 26 Outubro de 2011.

[10]]Zhengang Han, Weihua Li and Sirish L. Shah; *Fault detection and isolation in the presence of process uncertainties*; Elsevier, Control Engineering Practice 13, 2005, pag 587-599;

[11] Paul M. Frank, *Fault Diagnosis in Dynamic Systems Using Analytical and Knowledge-based Redundancy A Survey and Some New Results*, Automatica, Vol. 26, No. 3, pp. 459-474, 1990;

[12] Alexandre Carlos Eduardo; *Diagnóstico de Defeitos em Sistemas Mecânicos Rotativos através da Análise de Correlações e Redes Neurais Artificiais*, Tese de doutorado apresentada à Comissão de Pós-Graduação da Faculdade de Engenharia Mecânica, como requisito para a obtenção do título de Doutor em Engenharia Mecânica. Campinas, 2003, S.P. - Brasil.

[13] VibroSystM. *Zoom 5 Software Guia do Usuário*. P/N: 9476-26M1A-100. VibroSystM Inc. 2005.

[14] Aguirre, L. A., *Introdução à Identificação de Sistemas*, 2ª edição, UFMG, 2004.

[15] Karl J. Aström and Björn Wittenmark, Computer *Controlled Systems*, Prentice-Hall, 1984.

[16] L. X. Wang, *A course in Fuzzy Systems and Control*, Prentice-Hall International, Inc.,1997,

[17] Norberto Bramatti. *Desenvolvimento e Implantação de um Sistema de Monitoração on-line de Compensadores Síncronos*. Dissertação de Mestrado. Universidade Federal do Pará, Centro Tecnológico, Programa de Pós-graduação em Engenharia Elétrica. 2002.

[18] Lennart Ljung, *System Identification - Theory for the User*, PTR Prentice Hall, Englewood Cliffs, New Jersey, 1987;

[19] Lennart Ljung; *System Identification Tolbox 7 User's Guide*.

[20] Jang, J.-S. R., *ANFIS: Adaptive-Network-based Fuzzy Inference Systems*, *IEEE Transactions on Systems, Man, and Cybernetics*, Vol. 23, No. 3, pp. 665-685, May 1993.

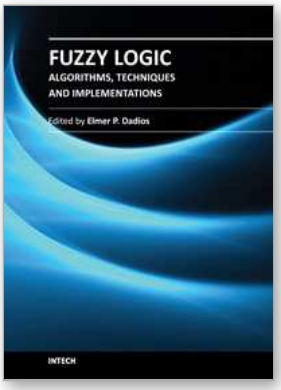

Fuzzy Logic - Algorithms, Techniques and Implementations
Edited by Prof. Elmer Dadios

ISBN 978-953-51-0393-6
Hard cover, 294 pages
Publisher InTech
Published online 28, March, 2012
Published in print edition March, 2012

Fuzzy Logic is becoming an essential method of solving problems in all domains. It gives tremendous impact on the design of autonomous intelligent systems. The purpose of this book is to introduce Hybrid Algorithms, Techniques, and Implementations of Fuzzy Logic. The book consists of thirteen chapters highlighting models and principles of fuzzy logic and issues on its techniques and implementations. The intended readers of this book are engineers, researchers, and graduate students interested in fuzzy logic systems.

How to reference
In order to correctly reference this scholarly work, feel free to copy and paste the following:

Marcelo Nascimento Moutinho (2012). Fault Diagnostic of Rotating Machines Based on Artificial Intelligence: Case Studies of the Centrais Elétricas do Norte do Brazil S/A – Eletrobras-Eletronorte, Fuzzy Logic - Algorithms, Techniques and Implementations, Prof. Elmer Dadios (Ed.), ISBN: 978-953-51-0393-6, InTech, Available from: http://www.intechopen.com/books/fuzzy-logic-algorithms-techniques-and-implementations/fault-diagnostic-of-rotating-machines-based-on-artificial-intelligence-case-studies-of-the-centrais-

INTECH
open science | open minds

InTech Europe
University Campus STeP Ri
Slavka Krautzeka 83/A
51000 Rijeka, Croatia
Phone: +385 (51) 770 447
Fax: +385 (51) 686 166
www.intechopen.com

InTech China
Unit 405, Office Block, Hotel Equatorial Shanghai
No.65, Yan An Road (West), Shanghai, 200040, China
中国上海市延安西路65号上海国际贵都大饭店办公楼405单元
Phone: +86-21-62489820
Fax: +86-21-62489821